Organic Electronics 122 (2023) 106887

Contents lists available at ScienceDirect

Organic Electronics

journal homepage: www.elsevier.com/locate/orgel

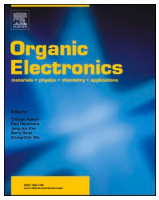

# Isotropic contact patterning to improve reproducibility in organic thin-film transistors

Stefano Lai [a,*], Katarina Kumpf [b], Pier Carlo Ricci [c], Philipp Fruhmann [b], Johannes Bintinger [d], Annalisa Bonfiglio [a], Piero Cosseddu [a]

[a] Department of Electrical and Electronic Engineering, University of Cagliari, Piazza d'Armi, 09123, Cagliari, Italy
[b] CEST – Center for Electrochemical Surface Technology, 2700, Wr. Neustadt, Austria
[c] Department of Physics, University of Cagliari, Complesso Universitario di Monserrato S.P, Monserrato-Sestu Km 0,700, 09042, Monserrato, Italy
[d] Biosensor Technologies, Austrian Institute of Technology, 3430, Tulln, Austria

ARTICLE INFO

*Keywords:*
Organic field-effect transistors
Organic semiconductor
Performance reproducibility
Meniscus-assisted printing

ABSTRACT

A novel approach for improving reproducibility of Organic Field-Effect Transistors electrical performances is proposed. The introduction of isotropic features in the layout of source and drain electrodes is employed to minimize the impact of randomly-distributed crystalline domains in the organic semiconductor film on the reproducibility of basic electrical parameters, such as threshold voltage and charge carrier mobility. A significant reduction of the standard deviation of these parameters is reported over a statistically-relevant set of devices with drop-casted semiconductor, if compared with results obtained in a standard, interdigitated transistor structure. A correlation between electrodes patterning and proposed result is demonstrated by deepening the analysis with the contribution of meniscus-assisted semiconductor printing, in order to precisely control the growth direction of crystals.

## 1. Introduction

In the last years, the interest towards flexible electronics is progressively shifting from basic research to industrial applications. Indeed, the possibility of fabricating flexible electronic devices with cost-efficient processes is paving the way for several applications ranging from flexible and conformable photovoltaic modules, flexible, foldable and rollable displays, to flexible sensors that could potentially be easily integrated into garments in order to create smart wearable systems [1]. Among all possible choices, organic materials have gained huge consideration not only for their peculiar electro-mechanical properties, but also for the simple, cost-effective and large-area fabrication processes that can be employed. Nonetheless, several key challenges such as lifetime, performances and their reliability and reproducibility still need to be overcome before the technology can enter the consumer market.

The case of Organic Field-Effect Transistor (OFET) is representative in this sense. OFETs are fundamental building blocks in sensors [2], actuators [3] and electronic circuits for signal acquisition, conditioning and processing elaboration [4,5]. Although impressive progress regarding electrical performances [6,7] and durability [8] has been made, there are still reliability and reproducibility issues which have dramatically slowed down the actual industrial development of organic electronic products. Whilst fabrication processes for organic devices are progressively improving in terms of reliability, the deposition of the organic semiconductor still represents the main bottleneck for the full reproducibility of device performances. Indeed, basic electrical parameters (such as threshold voltage, charge carrier mobility, subthreshold slope) are strongly reliant on the morphological features of organic semiconductors thin films. Although they can be precisely controlled in physical vapor deposition methods over small areas, their assessment is less trivial for solution processing techniques, which are normally preferred in terms of scalability, cost effectiveness and large area applications [9].

So far, most of efforts have been devoted in the development of strategies for improving the reproducibility of morphological properties of solution processed organic semiconductors, in particular for those that normally form polycrystalline films after the deposition. The main goal is to ensure crystalline alignment along the channel length direction in order to maximize charge transfer from source to drain. Different approaches have been proposed in literature for achieving this result:

* Corresponding author.
*E-mail address:* stefano.lai@unica.it (S. Lai).

https://doi.org/10.1016/j.orgel.2023.106887
Received 6 February 2023; Received in revised form 16 May 2023; Accepted 30 June 2023
Available online 3 July 2023

solution shearing (by means of bar/doctor blade coating systems or other inkjet printing equipment) is definitely the most widely used [10–14], but also the control of solvent evaporation [15,16] and OSC confinement [17,18] have been explored. Other approaches include the optimization of standard techniques, such as dip coating and spin coating, in order to control crystal direction [19,20], and the employment of temperature gradient [21], electric fields [22] and vibration/sound [23] to define preferential direction during crystal growth. Nonetheless, the best results at the state-of-the-art have been indeed demonstrated on planar, rigid substrates, since the greater surface roughness of flexible, plastic substrate leads to a high concentration of pinning sites that generally induces defects and thus leads to small and defective crystalline domains [24,25].

In this paper, we propose a novel approach, based on the introduction of isotropic features by patterning source and drain contacts in a spiral shape. This structure allows dramatically reducing the impact of random distribution of crystalline domains of a drop-casted organic semiconductor film on recorded device performances. As a consequence, a significant improvement of performance reproducibility, as well as an increase of charge carrier mobility, is achieved for spiral-shaped source and drain electrodes with respect to a standard interdigitated layout. In order to give a deeper insight into the mechanism, a deposition technique that provides control over the direction of the organic crystals, namely meniscus-guided printing, is employed, thus providing a complete picture on the relationship between alignment of crystalline domains and channel geometry.

## 2. Materials and methods

In order to demonstrate the feasibility of the approach, two different OFET structures have been fabricated (Fig. 1): a standard interdigitated device structure (i-OFET), and an isotropic OFET with concentric, spiral-shaped source and drain electrodes (s-OFET). Device fabrication has been carried out on 175 μm-thick polyethylene terephthalate (PET) foil, purchased by Goodfellow. The gate electrode has been patterned from a thermally evaporated aluminum film (under a pressure of $10^{-5}$ Torr) by a standard photolithographic process. The gate dielectric was a thin double layer composed by aluminum oxide (8 nm), thermally grown in oven at 50 °C for 12 h, and Parylene C (150 nm), deposited by Chemical Vapor Deposition (CVD) using a PDS2010 Labcoater 2 (Specialty Coating Systems). The capacitance per unit area of this double layer (15 nFcm$^{-2}$) allows devices to operate at low voltages [26]. Source and drain are patterned by a standard photolithographic process. The aspect ratio of both i-OFETs and s-OFETs is W/L = 300 (channel length of 40 μm). In particular, the channel width of s-OFETs was fixed using the well-known formula for Archimedean spiral roll length,

$$W = \frac{\pi N(D+d)}{2}$$

where $N$ is the number of turns, $d$ and $D$ are inner and outer diameters of the spiral, respectively. This information was then used to fix the channel width of i-OFETs, in order to ensure an identical aspect ratio.

In this study we have employed a well-known solution processable organic semiconductor capable to give rise to polycrystalline thin films with relatively large crystal domains, namely 6,13-Bis(triisopropylsilylethynyl)pentacene (TIPS pentacene, Sigma-Aldrich). Two different deposition techniques have been employed in this study. The first one is drop casting from a 1 wt% solution in anisole anhydrous (Sigma Aldrich). The second one is a meniscus-guided printing technique using a Nordson EFD E2 pneumatic nozzle printer and pressure controller Ultimus V with a custom-made heat plate to control substrate temperature. Before the printing, all devices were washed with water and ethanol and then dried under a $N_2$ stream. A syringe and a needle (300 μm in diameter) serve as the solution reservoir and the printing nozzle, respectively. A TIPS pentacene solution of 15 mg/mL was used and the reservoir is interfaced with Nordson EFD E3V pressure controller to provide vacuum-, forward pressure and a 3D-stage. Once the meniscus is created using a short forward pressure pulse (typically 10–20 ms; 4.48 kPa) vacuum (0.0 kPa) is applied and the needle is moved across the surface at a speed of 0.5 mm/s while maintaining a constant substrate temperature (55 °C). By adjusting the writing speed to match the solvent evaporation rate at the meniscus, organic crystals were anisotropically grown along the direction of nozzle movement [27]. A camera enabled alignment of different deposition layers. To minimize scratches, the print height was set to 130 μm and to ensure a controlled evaporation process, all devices were printed at a temperature of 55 °C.

The electrical characterization has been carried out by means of a Keithley SourceMeter® 2636 with custom Matlab® software in ambient conditions.

Absorption characterization has been performed in air with the PerkinElmer double beam Jasco V-750 UV/Vis Spectrophotometer in reflectivity mode, by using a sample without the TIPS as reference".

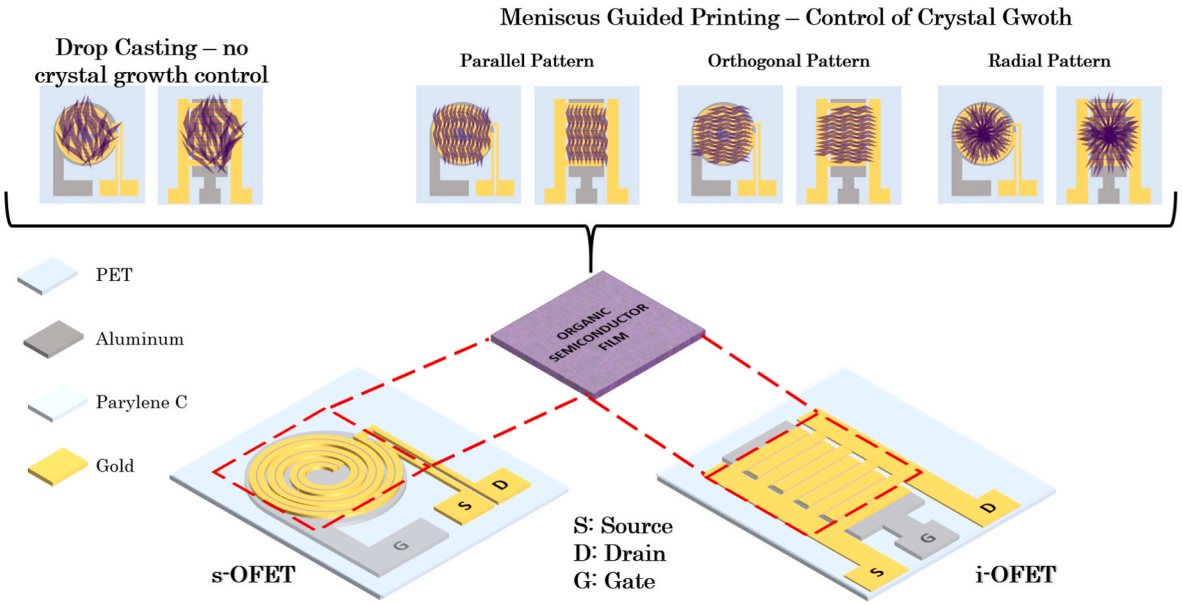


**Fig. 1.** a cartoon showing the s-OFET and i-OFET device structures with materials palette and the different organic semiconductor patterns tested.

Atomic Force Microscopy measurements were obtained by means of a SPM SOLVER PRO by NT-MDT in semi-contact mode using NT-MDT NSG01 tips.

## 3. Results and discussion

### 3.1. Reproducibility of device performance for drop-casted devices

First, the performances of devices fabricated by drop casting where evaluated to assess the effectiveness of the patterning approach for source and drain contacts. Thirty devices for each kind of layout have been fabricated in two different batches: each batch is composed by 15 i-OFETs and 15 s-OFETs fabricated on the same substrate (total dimension $5 \times 6$ cm$^2$) in order to keep a consistent comparison between the two solutions, and also to evaluate the process reliability in multiple batches. Typical output and transfer characteristic curves are shown in Fig. S1 (see Supporting Information). A total of 27 devices for each structure was considered, as three devices per structure were excluded from statistical analysis as defects in source/drain patterning resulted in a reduced aspect ratio with respect to the nominal one.

A statistical evaluation on two basic electrical parameters, namely threshold voltage ($V_{TH}$) and charge-carrier mobility ($\mu$), has been carried out on batches of both types of device structure. Threshold voltage and charge carrier mobility were extracted using the well-known linearization method of the square-root of the transfer characteristic curve in saturation regime [28]. Fig. 2 shows histograms of the value distribution for each of these parameters, comparing those extracted from i-OFETs (black) and s-OFETs (grey).

The average value of the threshold voltage (Fig. 2a) is around 0 V and comparable between i-OFETs and s-OFETs: this is coherent with the fact that gate-insulator-semiconductor structure is the same in the two layouts, and that overall device dimensions are the same. Interestingly enough, the 1-σ band of the distribution is four times narrower in s-OFETs (0.08 V vs. 0.32 V in i-OFETs), with 19 devices over 47 (70%) falling in the range [−0.5:0] V, and 13 (48%) in the range [−0.1:0] V. Moreover, a noteworthy increase of the charge carrier mobility was obtained (from 0.11 cm$^2$V$^{-1}$s$^{-1}$ in i-OFETs to 0.16 cm$^2$V$^{-1}$s$^{-1}$ in s-OFETs, Fig. 2b), thus proving that the isotropic layout is actually capable to maximize charge carrier collection. Moreover, a larger reproducibility of the charge carrier mobility values was obtained: the ratio between standard deviation and average value (variability coefficient [29]) denotates a 1-σ band more than halved (12% vs. 27%) in s-OFETs.

The enhanced reproducibility of both parameters can be attributed to the improved charge collection using the isotropic features of source and drain electrodes. Several studies report on the relationship of threshold voltage and mobility value and reproducibility and anisotropic charge transport in organic polycrystalline films, which depends both on intrinsic crystal structure and to the film arrangement at the macro-scale [30,31]. It is also well known that charge transport in OSCs occurs perpendicular to the molecular plane and that the electronic performance (mobility) scales with the degree of crystallinity. Hence, ideal printed OFET devices combine (semi-)crystalline features with scalable yet locally confined deposition techniques. Here, the spiral-shaped structure ensures a limitation in the anisotropic charge transport in the semiconductor film, thus reducing the variability of electrical performances among different devices, even if the morphological features of the semiconductor film vary. Interestingly enough, the value of the threshold voltage is not significantly modified by the employment of an isotropic electrode configuration, probably because the material stacking and the morphological features are similar in i-OFETs and s-OFETs. The increase of the charge carrier mobility by up to 45% could confirm the capability of electrodes to better collect charge carriers from randomly oriented crystals, thus improving charge transport through electrodes.

In order to put weight on this discussion, a systematic evaluation of other parameters that may explain an enhancement of electrical performances was carried out. Crystalline properties and morphology of the drop-casted TIPS pentacene layer on i-OFETs and s-OFETs where characterized by means of UV/Vis spectroscopy and AFM. No significant difference between absorption spectra in the two kinds of devices was observed (Fig. S2 in Supplementary Information): characteristic absorption peaks of TIPS pentacene in its crystalline form (600 nm, 650 nm, 700 nm [32]) were found in absorption spectra. Similarly, also crystalline dimensions and characteristics resulted comparable in i-OFETs and s-OFETs from AFM analysis (Fig. S3 in Supplementary Information). Moreover, contact resistance in the two layouts was evaluated by means of Y-method function [33] (details in Supplementary information): a value of $R_CW$ of $(7.3 \pm 1.5)\cdot 10^5$ Ω cm and $(7.1 \pm 1.1)\cdot 10^5$ Ω cm have been obtained for i-OFETs and s-OFETs, respectively. These values are consistent with previous literature about TIPS pentacene/bare gold interfaces [34,35], and demonstrate that modification in the contact resistance can't justify the improved electrical performances obtained in s-OFETs.

### 3.2. Validation of result by means of meniscus-guided OSC patterning

In order to verify the previous hypotheses and validate the effectiveness of the proposed approach, an intentional isotropy in crystal growth has been produced on i-OFET and s-OFET by means of meniscus-assisted printing. This technique can control the crystallization of small

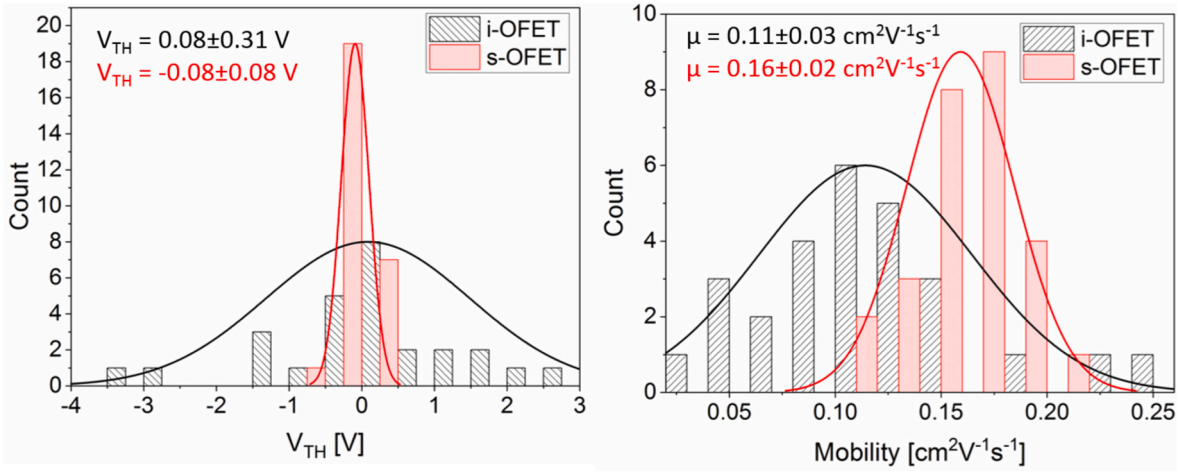


**Fig. 2.** histograms of threshold voltage (left) and mobility (right) values for i-OFETs (black) and s-OFETs (red) recorded in a batch of 27 device per typology. Average and standard deviation value are reported as inset.

molecule organic semiconductor thin films during deposition (Fig. S4 in Supplementary Information). The term "meniscus-guided" refers to the fact that a meniscus is translated across a substrate by virtue of a coating head or viscous forces, in effect guiding and controlling film deposition. Three different patterns have been employed, as shown in Fig. 1. In the first one, namely parallel, the crystals have been induced to grown parallel to the channel length of the i-OFET configuration. A second one, exhibits orthogonally directed crystals parallel to channel width in i-OFETs. Lastly, radial orientation of crystals ensured isotropic features which was achieved by arranging printed lines along the radius of a hypothetical circle centered at the origin point of the radial transistor configuration. Pictures of the three patterns have been reported on Fig. S5 in the Supporting Information.

The three patterns have been printed on both i-OFET and s-OFET structure. Fig. 3 shows the average value of charge carrier mobility on a set of 5 devices per type of transistor and pattern. In Supplementary Information, representative characteristic curves of the different patterns printed over i-OFETs and s-OFETs are reported (Figs. S6–S8). It is possible to observe that the best performance among i-OFETs has been obtained for the parallel pattern, as crystals are mainly aligned along the preferential direction for charge transfer between source and drain. In the orthogonal pattern, the charge carrier mobility drops as a consequence of the full misalignment between crystalline domains and charge transfer direction. In the case of radial pattern, the mobility is somehow intermediate between the two latter conditions, as a significant number of crystals have a direction compatible with an effective charge transfer from source to drain, no matter of the effective crystal direction. For s-OFETs, it is interesting to observe that there isn't a significant difference between parallel and orthogonal pattern: we hypothesize that this is related to the isotropic orientation of the channel length axis, which left the morphological characteristics of the two patterns unaffected. On the contrary, as an isotropic crystal orientation has been induced in the radial pattern, a significantly larger charge carrier mobility was observed. These results demonstrate that the isotropic characteristics of source and drain electrodes play a role in the way charge transfer occurs in a semiconductor film, and thus on the improved reproducibility and performances of organic devices.

## 4. Conclusions

In conclusion, a novel approach for ensuring an enhanced reproducibility of OFET electrical performances based on isotropic source/drain patterning is proposed. The OFET structure implementing this feature (s-OFET) shows basic device performances comparable with those of standard layouts (i-OFETs) fabricated with the same materials and processes, thus demonstrating that the isotropic patterning does not produce undesired effects of key transistor characteristics. Interestingly enough, a statistically-relevant comparison between s-OFETs and i-OFETs demonstrated that the proposed strategy leads to a significant reduction of the standard deviation in the value of basic electrical parameters. In addition, a significant increase of the charge carrier mobility has been observed, suggesting that the charge carrier collection in the channel is more effective in s-OFET. The effect of the introduction of an isotropic configuration of the contacts has been investigated by introducing anisotropic features in the semiconductor film by pneumatic nozzle-assisted printing, which allows for control over the direction of crystal growth. The proposed approach is thus able to improve device reliability and to optimize performances in devices fabricated with no control of crystal alignment in the OSC film, such as drop-casting Nonetheless, it is noteworthy that the proposed approach is not necessarily complementary to OSC patterning methods, as demonstrated by the successful integration with pneumatic printing. For instance, the employment of isotropic patterning of source/drain electrodes would mitigate misalignment problems in crystal orientation when performed on plastic substrates. Similarly, s-OFETs would further take advantage of the induction of high isotropic degree in crystal growth. Therefore, the proposed results can guide the development of innovative approaches for highly-reliable OFET fabrication by means of scalable techniques.

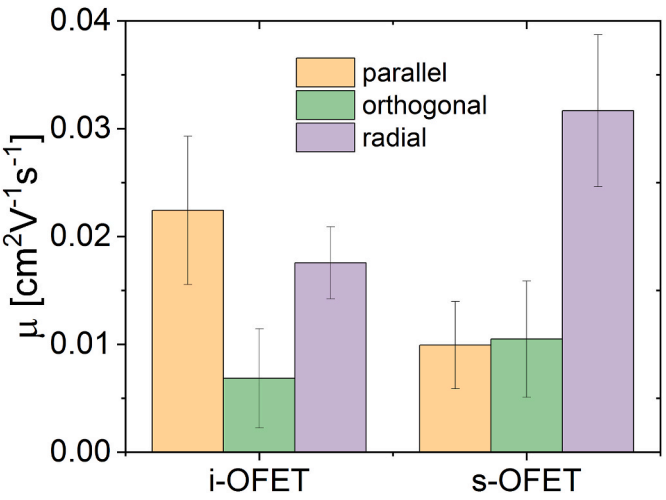


**Fig. 3.** average and standard deviation for charge carrier mobilities for the different meniscus-assisted printed OSC patterns in i-OFETs and s-OFETs.

## Declaration of competing interest

The authors declare that they have no known competing financial interests or personal relationships that could have appeared to influence the work reported in this paper.

## Data availability

Data will be made available on request.

## Acknowledgements

Philipp Fruhmann gratefully acknowledge the Gesellschaft für Forschungsförderung Niederösterrreich GmbH (GFF) for funding parts of this work within grant LSC19-013, and the Österreichische Forschungsförderungs GmbH (FFG) for funding the Centre of Electrochemical Surface Technology within the COMET program (grant-No.: 865864). Johannes Bintinger gratefully acknowledges funding from the Austrian Research Promotion Agency (FFG; PRECISE-SMELL #: 888067) as well as the financial support from the European Fund for Regional Development (EFRE) and the Fund for Economy and Tourism of Lower Austria. (grant #: WST3-F-5030665/005-2018 and grant #: WST3-F5030665/012-2021).

## Appendix A. Supplementary data

Supplementary data to this article can be found online at https://doi.org/10.1016/j.orgel.2023.106887.

## References

[1] K. Liu, B. Ouyang, X. Guo, Y. Guo, Y. Liu, Advances in flexible organic field-effect transistors and their applications for flexible electronics, npj Flex Electron 6 (2022) 1, https://doi.org/10.1038/s41528-022-00133-3.
[2] H. Li, W. Shi, J. Song, H.-J. Jang, J. Dailey, J. Yu, H.E. Katz, Chemical and biomolecule sensing with organic field-effect transistors, Chem. Rev. 119 (2019) 3–35, https://doi.org/10.1021/acs.chemrev.8b00016.
[3] T. Arbring Sjöström, M. Berggren, E.O. Gabrielsson, P. Janson, D.J. Poxson, M. Seitanidou, D.T. Simon, A decade of iontronic delivery devices, Adv. Mater. Technol. 3 (2018), 1700360, https://doi.org/10.1002/admt.201700360.
[4] P.C. Harikesh, C.-Y. Yang, D. Tu, J.Y. Gerasimov, A.M. Dar, A. Armada-Moreira, M. Massetti, R. Kroon, D. Bliman, R. Olsson, E. Stavrinidou, M. Berggren, S. Fabiano, Organic electrochemical neurons and synapses with ion mediated

spiking, Nat. Commun. 13 (2022) 901, https://doi.org/10.1038/s41467-022-28483-6.
[5] J.Y. Gerasimov, R. Gabrielsson, R. Forchheimer, E. Stavrinidou, D.T. Simon, M. Berggren, S. Fabiano, An evolvable organic electrochemical transistor for neuromorphic applications, Adv. Sci. 6 (2019), 1801339, https://doi.org/10.1002/advs.201801339.
[6] L. Luo, W. Huang, C. Yang, J. Zhang, Q. Zhang, Recent advances on π-conjugated polymers as active elements in high performance organic field-effect transistors, Front. Physiol. 16 (2021), 33500, https://doi.org/10.1007/s11467-020-1045-6.
[7] X. Ren, Z. Lu, X. Zhang, S. Grigorian, W. Deng, J. Jie, Low-voltage organic field-effect transistors: challenges, progress, and prospects, ACS Materials Lett 4 (2022) 1531–1546, https://doi.org/10.1021/acsmaterialslett.2c00440.
[8] J. Kimpel, T. Michinobu, Conjugated polymers for functional applications: lifetime and performance of polymeric organic semiconductors in organic field-effect transistors, Polym. Int. 70 (2021) 367–373, https://doi.org/10.1002/pi.6020.
[9] P. Andersson Ersman, R. Lassnig, J. Strandberg, D. Tu, V. Keshmiri, R. Forchheimer, S. Fabiano, G. Gustafsson, M. Berggren, All-printed large-scale integrated circuits based on organi electrochemical transistors, Nat. Commun. 10 (2019) 5053, https://doi.org/10.1038/s41467-019-13079-4.
[10] T. Kushida, T. Nagase, H. Naito, Mobility enhancement in solution-processable organic transistors through polymer chain alignment by roll-transfer printing, Org. Electron. 12 (2011) 2140–2143, https://doi.org/10.1016/j.orgel.2011.09.013.
[11] K. Kim, J. Bae, S.H. Noh, J. Jang, S.H. Kim, C.E. Park, Direct writing and aligning of small-molecule organic semiconductor crystals via “dragging mode” electrohydrodynamic jet printing for flexible organic field-effect transistor arrays, J. Phys. Chem. Lett. 8 (2017) 5492–5500, https://doi.org/10.1021/acs.jpclett.7b02590.
[12] S. Yang, S. Park, J. Bintinger, Y. Bonnassieux, J. Anthony, I. Kymissis, Employing pneumatic nozzle printing for controlling the crystal growth of small molecule organic semiconductor for field-effect transistors, Adv. Electron. Mater. 4 (2018), 1700534, https://doi.org/10.1002/aelm.201700534.
[13] X. Gu, L. Shaw, K. Gu, M.F. Toney, Z. Bao, The meniscus-guided deposition of semiconducting polymers, Nat. Commun. 9 (2018) 534, https://doi.org/10.1038/s41467-018-02833-9.
[14] S. Lai, I. Temiño, T. Cramer, F.G. del Pozo, B. Fraboni, P. Cosseddu, A. Bonfiglio, M. Mas-Torrent, Morphology influence on the mechanical stress response in bendable organic field-effect transistors with solution-processed semiconductors, Adv. Electron. Mater. 4 (2018), 1700271, https://doi.org/10.1002/aelm.201700271.
[15] H. Li, B.C.-K. Tee, J.J. Cha, Y. Cui, J.W. Chung, S.Y. Lee, Z. Bao, High-mobility field-effect transistors from large-area solution-grown aligned $C_{60}$ single crystals, J. Am. Chem. Soc. 134 (2012) 2760–2765, https://doi.org/10.1021/ja210430b.
[16] D. Bharti, V. Raghuwanshi, I. Varun, A.K. Mahato, S.P. Tiwar, Directional solvent vapor annealing for crystal alignment in solution-processed organic semiconductors, ACS Appl. Mater. Interfaces 9 (2017) 26226–26233, https://doi.org/10.1021/acsami.7b03432.
[17] A. Kumatani, C. Liu, Y. Li, P. Darmawan, K. Takimija, T. Minari, K. Tsukagoshi, Solution-processed, self-organized organic single crystal arrays with controlled crystal orientation, Sci. Rep. 2 (2012) 393, https://doi.org/10.1038/srep00393.
[18] G. Giri, S. Park, M. Vosgueritchian, M.M. Shulaker, Z. Bao, High-mobility, aligned crystalline domains of TIPS-pentacene with metastable polymorphs through lateral confinement of crystal growth, Adv. Mater. 26 (2014) 487–493, https://doi.org/10.1002/adma.201302439.
[19] N.-K. Kim, S.-Y. Jang, G. Pace, M. Caironi, W.-T. Park, D. Khim, J. Kim, D.-Y. Kim, Y.-Y. Noh, High-performance organic field-effect transistors with directionally aligned conjugated polymer film deposited from pre-aggregated solution, Chem. Mater. 27 (2015) 8345–8353, https://doi.org/10.1021/acs.chemmater.5b03775.
[20] J. Jang, S. Nam, K. Im, J. Hur, S.N. Cha, J. Kim, H.B. Son, H. Suh, M.A. Loth, J. E. Anthony, J.-J. Park, C.E. Park, J.M. Kim, K. Kim, Highly crystalline soluble acene crystal arrays for organic transistors: mechanism of crystal growth during dip-coating, Adv. Funct. Mater. 22 (2012) 1005–1014, https://doi.org/10.1002/adfm.201102284.
[21] Y. Diao, B.K. Tee, G. Giri, D.H. Kim, H.A. Becerril, R.M. Stoltenberg, T.H. Lee, G. Xue, S.C.B. Mannsfeld, Z. Bao, Solution coating of large-area organic semiconductor thin films with aligned single-crystalline domains, Nat. Mater. 12 (2013) 665–671, https://doi.org/10.1038/nmat3650.
[22] K. Kotsuki, S. Obata, K. Saiki, Self-aligned growth of organic semiconductor single crystals by electric field, Langmuir 32 (2016) 644–649, https://doi.org/10.1021/acs.langmuir.5b03975.
[23] P.J. Diemer, C.R. Lyle, Y. Mei, C. Sutton, M.M. Payne, J.E. Anthony, V. Coropceanu, J.-L. Brédas, O.D. Jurchescu, Vibration-assisted crystallization improves organic/dielectric interface in organic thin-film transistors, Adv. Mater. 25 (2013) 6956–6962, https://doi.org/10.1002/adma.201302838.
[24] Y.D. Park, J.A. Lim, H.S. Lee, K. Cho, Interface engineering in organic transistors, Mater. Today 10 (2007) 46–54, https://doi.org/10.1016/S1369-7021(07)70019-6.
[25] A.A. Virkar, S. Mannsfeld, Z. Bao, N. Stingelin, Organic semiconductor growth and morphology considerations for organic thin-film transistors, Adv. Mater. 22 (2010) 3857–3875, https://doi.org/10.1002/adma.200903193.
[26] P. Cosseddu, S. Lai, M. Barbaro, A. Bonfiglio, Ultra-low voltage, organic thin film transistors fabricated on plastic substrates by a highly reproducible process, Appl. Phys. Lett. 100 (2012), 093305, https://doi.org/10.1063/1.3691181.
[27] S. Yang, S. Park, J. Bintinger, Y. Bonnassieux, I. Kymissis, P-99: pneumatic nozzle printing as a versatile approach to crystal growth management and patterning of printed organic thin film transistors, SID Symposium Digest of Technical Papers 47 (2016) 1502–1505, https://doi.org/10.1002/sdtp.10983.
[28] G. Horowitz, P. Lang, M. Mottaghi, H. Aubin, Extracting parameters from the current–voltage characteristics of organic field-effect transistors, Adv. Funct. Mater. 14 (2004) 1069, https://doi.org/10.1002/adfm.200305122.
[29] W. Deng, H.M. Lei, X.J. Zhang, F.M. Sheng, J.L. Shi, X.L. Zhang, X.Y. Liu, S. Grigorian, X.H. Zhang, J.S. Jie, Scalable growth of organic single-crystal films via an orientation filter funnel for high-performance transistors with excellent uniformity, Adv. Mater. 34 (2022), 2109818, https://doi.org/10.1002/adma.202109818.
[30] J. Chen, C.K. Tee, M. Shtein, D.C. Martin, J. Anthony, Controlled solution deposition and systematic study of charge-transport anisotropy in single crystal and single-crystal textured TIPS pentacene thin films, Org. Electron. 10 (2009) 696–703, https://doi.org/10.1016/j.orgel.2009.03.007.
[31] G. Lu, J. Chen, W. Xu, S. Li, X. Yang, Aligned polythiophene and its blend film by direct-writing for anisotropic charge transport, Adv. Funct. Mater. 24 (2014) 4959–4968, https://doi.org/10.1002/adfm.201400699.
[32] D.A. Kadri, D.A. Karim, M. Seck, K. Diouma, M. Pasquinelli, Optimization of 6, 13Bis (triisopropylsilylethynyl) pentacene (TIPS-Pentacene) organic field effect transistor: annealing temperature and solvent effects, Mater. Sci. Appl. 9 (2018) 900–912, https://doi.org/10.4236/msa.2018.911065.
[33] Y. Xu, T. Minari, K. Tsukagoshi, J.A. Chroboczek, G. Ghibaudo, Direct evaluation of low-field mobility and access resistance in pentacene field-effect transistors, J. Appl. Phys. 107 (2010), 114507, https://doi.org/10.1063/1.3432716.
[34] S. Choi, C. Fuentes-Hernandez, C.-Y. Wang, T.M. Khan, F.A. Larrain, Y. Zhang, S. Barlow, S.R. Marder, B. Kippelen, A study on reducing contact resistance in solution-processed organic field-effect transistors, ACS Appl. Mater. Interfaces 8 (2016) 24744–24752, https://doi.org/10.1021/acsami.6b07029.
[35] D. Boudinet, M. Benwadih, Y. Qi, S. Altazin, J.-M. Verilhac, M. Kroger, C. Serbutoviez, R. Gwoziecki, R. Coppard, G. Le Blevennec, A. Kahn, G. Horowitz, Modification of gold source and drain electrodes by self-assembled monolayer in staggered n- and p-channel organic thin film transistors, Org. Electron. 11 (2010) 227–237, https://doi.org/10.1016/j.orgel.2009.10.021.